EFFECTIVE FORCE TESTING: A METHOD OF SEISMIC SIMULATION FOR STRUCTURAL TESTING

By J. Dimig,[1] C. Shield,[2] C. French,[3] F. Bailey,[4] and A. Clark[5]

ABSTRACT: This paper presents a test method for real-time earthquake simulation studies of large scale test structures. The method, effective force testing (EFT), is based on a force control algorithm. For systems that can be modeled as a series of lumped masses (e.g., frame structures where masses are assumed lumped at the floor levels), the EFT forces are known a priori for any acceleration record. As opposed to the pseudodynamic test method (a displacement-based control procedure), there is no computational time required for the EFT method in determining the required force signal; it is known prior to the test once the structural mass and ground acceleration record to be simulated are determined. Research has been conducted on a single-degree-of-freedom system at the University of Minnesota to investigate the potential of the EFT method. A direct application of the method was found ineffective because the actuator was unable to apply force at the natural frequency of the structure owing to actuator/control/structure interaction. However, numerical simulations and experimental implementation indicated that an additional velocity feedback loop incorporated into the control system can overcome this problem while maintaining the ability to do real-time testing.

BACKGROUND

There are three primary types of test methods used to investigate the performance of structural systems subjected to seismic loadings (Clark et al. 1989). They are earthquake simulation studies on shake tables, quasi-static cyclic studies of components, and pseudodynamic test methods (Moehle 1996). Each of these methods has advantages and disadvantages. For example with shake table studies, test structures may be subjected to actual earthquake acceleration records to investigate dynamic effects; however, the size of the structure is limited or scaled by the capacity of the shake table. At smaller scales, it is difficult to investigate reinforcement details, bond, shear, and anchorage because these phenomena do not scale well. In addition to possible scaling limitations, control problems may include undesirable pitching of the shake table from the applied motions. Quasi-static cyclic studies of components offer the advantage of investigating actual details. However, effects associated with the dynamic nature of earthquakes are not captured in these tests. The demands on the elements may not simulate those imposed in an actual earthquake. The pseudodynamic method enables testing of large structures (details, bond, shear, anchorage), and the loading history is intended to simulate an actual earthquake. The dynamic effects, however, are difficult to simulate with the pseudodynamic test method because a displacement control algorithm is used. The imposed deformations are not known a priori. For this test method, the imposed displacements depend on the response of the structure; they are a function of the structural stiffness, which changes as the structure is damaged. Pseudodynamic testing at near real time presents a problem if the structure develops real inertial and damping forces, because these forces are already accounted for in the loading algorithm. The effective force testing (EFT) method, described in this paper, represents a fourth type of seismic testing. The main advantage of the EFT method is the ability to perform real-time earthquake simulation because the forces are known a priori.

DESCRIPTION OF EFT METHOD

The concept of the effective force method is based on a transformation of coordinates. The response of a system to a given ground motion may be replicated by applying an effective force ($-m\ddot{x}_g$) to the mass of the system. Fig. 1(a) shows a single-degree-of-freedom (SDOF) system subjected to a base motion, $\ddot{x}_g$. The following equation of motion may be obtained for this system:

$$m\ddot{x}_a + c\dot{x} + kx = 0 \tag{1}$$

where m is the mass of the system, c is the viscous damping coefficient, and k is the system stiffness. Subscript a refers to motion relative to a fixed reference frame (absolute displacement). Motions of the mass relative to the ground are nonsubscripted.

The absolute displacement of the system mass consists of the displacement of the mass with respect to the ground and the ground displacement:

$$x_a = x + x_g \tag{2}$$

Coordinate transformation of the acceleration results in

$$\ddot{x}_a + \ddot{x} + \ddot{x}_g \tag{3}$$

Combining (1) and (3) yields

$$m\ddot{x} + c\dot{x} + kx = -m\ddot{x}_g = P_{\text{eff}}(t) \tag{4}$$

For a SDOF system, the mass multiplied by the ground acceleration is equivalent to an ''effective force,'' $P_{\text{eff}}(t)$, applied to the mass in a fixed reference frame (Clough 1975; Chopra 1995).

The proposed technique uses the same setup as pseudodynamic testing [i.e., test structure fixed to the ground, and all motions measured relative to the ground, Fig. 1(b)], and restrictions on the type of structure that can be tested are similar to those required by the pseudodynamic test method (i.e., structure can be idealized as a lumped mass system). The effective force ($-m\ddot{x}_g$) to be applied to the structure, in the EFT method, is a function of the mass of the structure, which is typically known or can be estimated with good accuracy before testing, and the earthquake ground acceleration record to be used. Consequently, the force-control loading history ($-m\ddot{x}_g$) is known a priori for any earthquake acceleration record. The effective force time history is a function only of the

[1]Struct. Engr., Wiss Janney Elstner & Associates.
[2]Assoc. Prof., Dept. of Civ. Engrg., Univ. of Minnesota, Minneapolis, MN 55455.
[3]Prof., Dept. of Civ. Engrg., Univ. of Minnesota, Minneapolis, MN.
[4]Prof., Dept. of Elec. Engrg., Univ. of Minnesota, Minneapolis, MN.
[5]Engr., Advanced Systems Division, MTS Systems Corp.

Note. Associate Editor: Sashi K. Kunnath. Discussion open until February 1, 2000. To extend the closing date one month, a written request must be filed with the ASCE Manager of Journals. The manuscript for this paper was submitted for review and possible publication on September 19, 1996. This paper is part of the ***Journal of Structural Engineering***, Vol. 125, No. 9, September, 1999. ©ASCE, ISSN 0733-9445/99/0009-1028–1037/$8.00 + $.50 per page. Paper No. 14172.

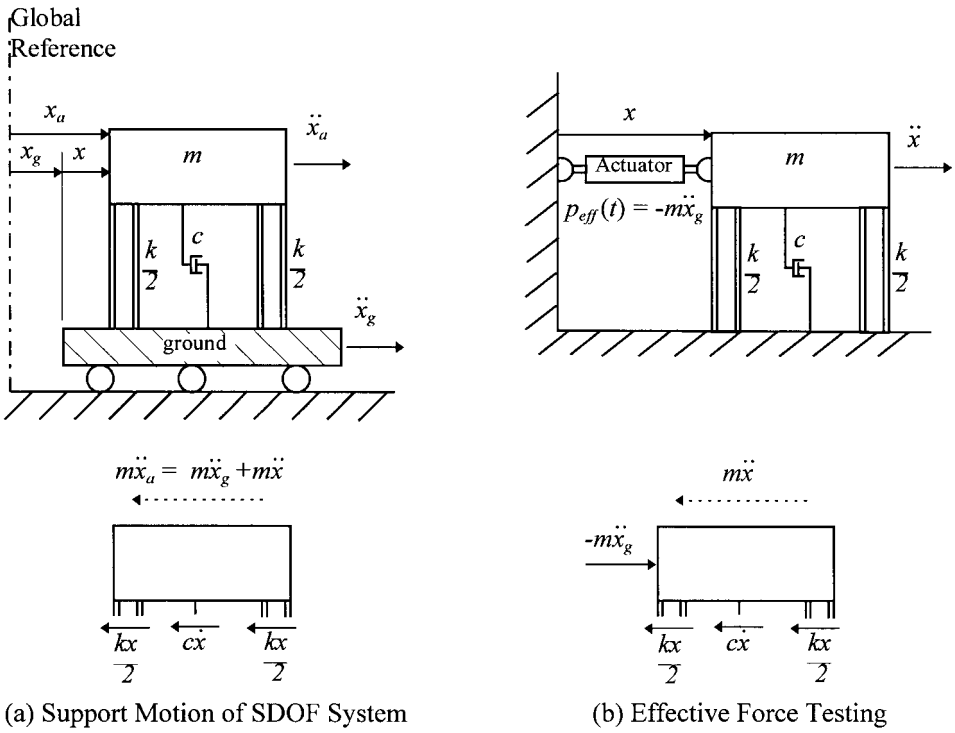

FIG. 1. Development of Effective Force Testing (EFT) Method

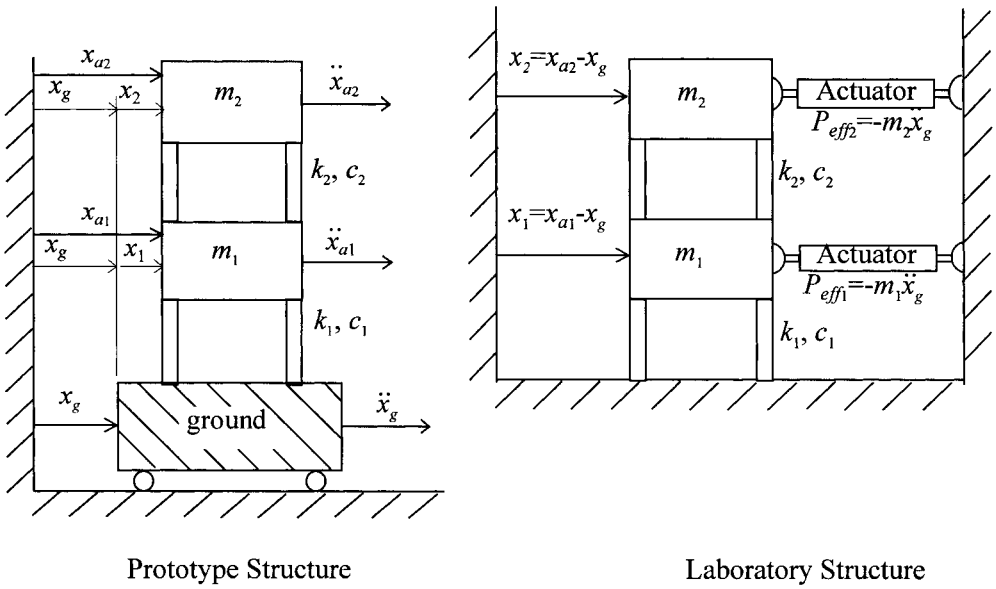

FIG. 2. Application of EFT to MDOF Systems

structural mass and ground acceleration history; it is not affected by the structural response (linear or nonlinear behavior).

Theoretically, the EFT method can be applied directly to test systems with nonlinear stiffness and damping mechanisms. As the structural system stiffness and damping change, the structural response will be affected, but the applied effective force will not be affected, as shown by (4). No structural parameters (stiffness or damping) are needed to determine the effective (applied) force.

A theoretical extension of the effective force technique to multiple-degree-of-freedom (MDOF) systems is illustrated in Fig. 2. In this case, an effective force is applied to each level (lumped mass) of the structure. The forces at each level are equal to the mass at that level multiplied by the ground acceleration. Therefore even for the case of an MDOF system, all of the applied effective forces are known before the test begins.

The concept of EFT is not new. It has been described in papers discussing the pseudodynamic test method (Mahin and Shing 1985; Mahin et al. 1989; Thewalt and Mahin 1987). These papers present the possibility of using a pseudodynamic test setup with explicit time-varying forces imposed at each lumped mass to conduct real-time tests without the need for computing and imposing required displacements. Because of the lack of displacement control and required integration algorithms, the technique is conceptually and physically different from ''real-time pseudodynamic testing'' (Nakashima et al. 1992).

While the testing scheme is conceptually simple, its implementation has been considered to be problematic. Thewalt and

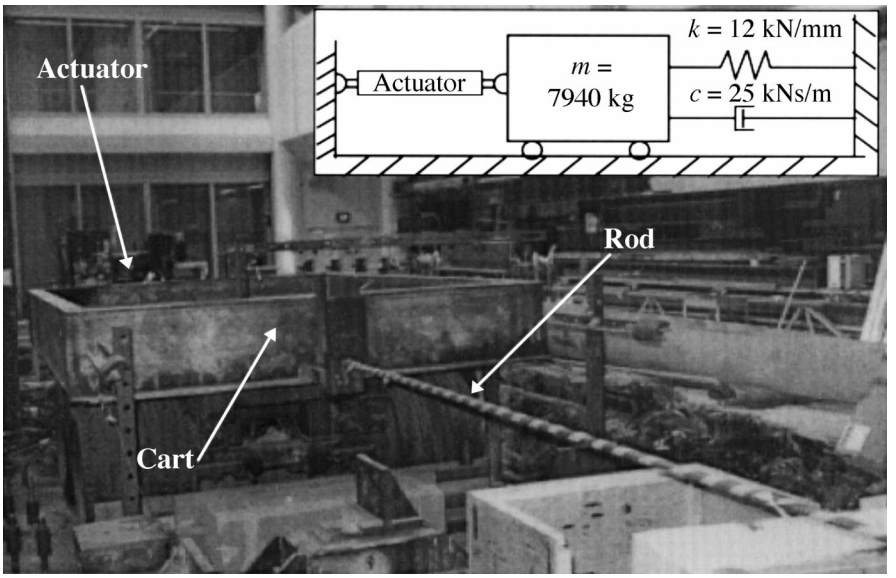

FIG. 3. Test Setup of SDOF Model

Mahin (1987) stated that the technique requires high-quality controllers and servovalves, but the total test control problem may be simpler than that of a shake table. Although in an unpublished study in 1987 (''Development and evaluation of the pseudodynamic test method'') Mahin indicated that shake table testing is probably more practical given both the power supply capacity and the relative displacements required of the degree of freedom masses, in the case of equal structural deformation response, the energy input to the structure would be expected to be the same for the two testing techniques. In fact there is potential for laboratory energy and power savings for EFT because there is no shake table to be moved. As far as the authors know, no previous experimental work has been conducted on the EFT method.

EXPERIMENTAL INVESTIGATION OF EFT METHOD

To investigate the feasibility of this method of testing, including power and control algorithm requirements, a SDOF system was constructed in the laboratory at the University of Minnesota. For demonstration purposes, the system presented in this paper was a linear-elastic SDOF structure, although, as noted in the previous section, this is not a requirement for the EFT test method to be applicable. The mass-spring-damper system, shown schematically (inset) and in a photograph in Fig. 3, consisted of a cart of mass 7,940 kg (17,500 lb), and a 25 mm (1 in.), 1,030 MPa (150 ksi) rod that served as a spring. The rod was pretensioned to 67 kN (15 kip) to prevent possible buckling. The properties of the system were investigated through a series of free and forced sinusoidal vibrations and static loading. The measured stiffness, natural frequency, and system damping ratio were found to be 11.8 kN/mm (67.1 k/in.), 6.2 Hz, and 2%, respectively. The force needed to overcome static friction was under 900 N (200 lb); hence the majority of the damping was deemed to be viscous, coming from the connections to the cart, as well as suspension/bearings of the cart.

An ''effective force'' was applied to the lumped mass (cart) using a hydraulic actuator by supplying the effective force time series as the command signal to the actuator controller. In the course of the investigation, the actuator servovalve was changed to investigate the effect of different flow capacities on the response. Three systems were used: (1) a 340 kN (77 kip) actuator with a two-stage 0.95 L/s (15 gpm) servovalve; (2) a 340 kN (77 kip) actuator with a two-stage 1.9 L/s (30 gpm) servovalve; and (3) a 340 kN (77 kip) actuator with a three-stage 5.7 L/s (90 gpm) servovalve.

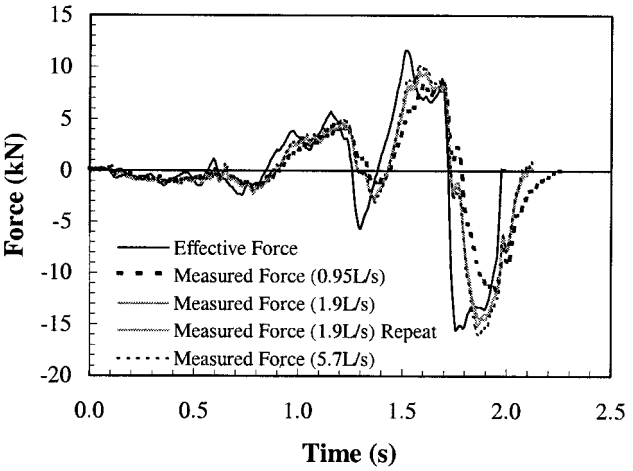

FIG. 4. Effective Force Command

The servohydraulic system was controlled by a computerized digital-to-analog converter that was used to input earthquake motions to the actuator. Entire earthquake records, two second and five second segments of earthquake records (for greater detail), and sinusoidal waves were used as input ground motions in determining the effective forces to be applied to the SDOF test structure. This paper presents the results for two of the earthquake segments investigated (2 and 5 s of the 1940 El Centro N-S ground motion). Similar observations and conclusions were obtained from the other tests (Murcek 1996).

The feasibility of the EFT method can be investigated by comparing the input effective force function (command signal) with the force measured from the actuator load cell. The input force is the force expected to be applied by the actuator. The earthquake effective force function segments ($-m\ddot{x}_g$) are shown in Fig. 4. Superimposed on Fig. 4 are the forces measured by the load cell in the 340 kN (77 kip) actuator attached to the cart. The results are shown for all three servovalves for the 2 s El Centro segment. The similarity of the force measured in the actuator to the input function demonstrates the potential of the EFT method. It is evident in Fig. 4, however, that the 1.9 L/s (30 gpm) and 5.7 L/s (90 gpm) systems were better able to follow the input signal, although all measured

forces show a time lag with respect to the input effective force function.

Servovalve Requirements

The required flow capacity of the servovalves can be determined by comparing the power requirements of the applied motion with the force-velocity curves that define the theoretical limitations of the servohydraulic systems used, as shown in Fig. 5. The curves are based on design equations developed to predict the performance of a given servohydraulic system (Clark 1983). The force capacity of an actuator, f, as a function of velocity, v, may be written as

$$f(v) = \text{sgn}(v) f_{\max} \left(1 - \frac{1}{\alpha^2} \frac{v^2}{v_{\max}^2}\right) \quad (5)$$

where $f_{\max}$ is the rated maximum actuator force with full effective supply pressure drop across the actuator piston, α is the servovalve spool opening (1.0 equals 100% open), and $v_{\max}$ is the maximum velocity with full effective pressure drop across the servovalve, which may be calculated as

$$v_{\max} = \frac{k_s}{A} \sqrt{\frac{p_s}{p_d}} \quad (6)$$

where k_s is the servovalve flow rating, A is the actuator piston area, p_s is the hydraulic supply pressure, and p_d is the servovalve pressure drop rating. To be conservative, a maximum spool opening of 80% ($\alpha = 0.8$) was assumed. The force-velocity demands of a given motion must remain within these envelopes to ensure that the hydraulic system can provide adequate power. The actuator velocity required to apply the El Centro input force function to the SDOF system was determined using a piecewise-linear analysis of the loading function. Approximately 1.75 s into the loading function, the power requirements are observed to extend beyond the capabilities of the 340 kN (77 kip) actuator with a 0.95 L/s (15 gpm) servovalve (Fig. 5). The power requirements stay within the capabilities of the 340 kN (77 kip) actuator with a 1.9 L/s (30 gpm) servovalve throughout the entire 2 s loading function. This explains why the 1.9 L/s (30 gpm) and 5.7 L/s (90 gpm) servovalve systems were better able to apply the force demanded by the input effective force signal shown in Fig. 4. However, for longer segments of El Centro, the power requirements fell outside of the 1.9 L/s (30 gpm) envelope; hence for the remainder of this study, only the 5.7 L/s (90 gpm) servovalve was used.

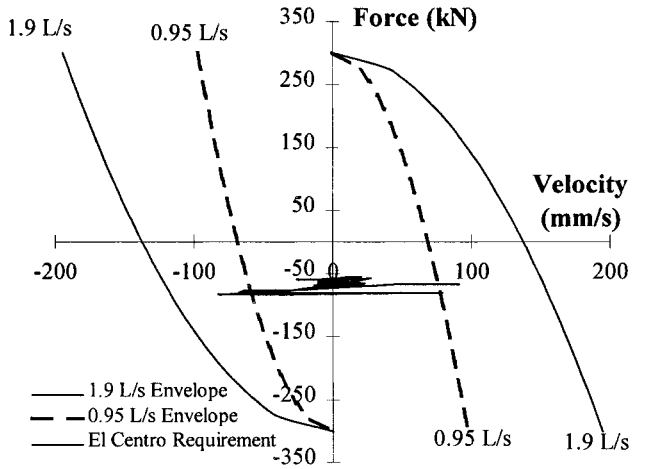

FIG. 5. Force-Velocity Requirements of the Actuator for Applying Effective Force El Centro Segment

Testing Requirements

In conducting earthquake simulation tests, it is not necessary for the recorded earthquake motions to be exactly replicated. Rather, some of the most important features of an earthquake simulation test are repeatability, reproducibility, and replication of the correct frequency content of the earthquake signal

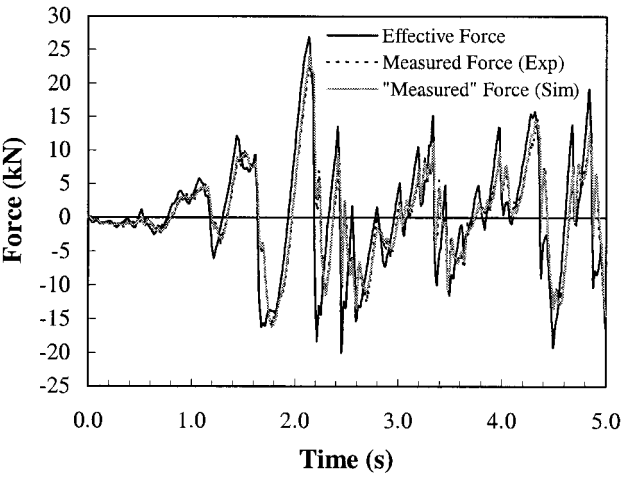

(a) Effective force

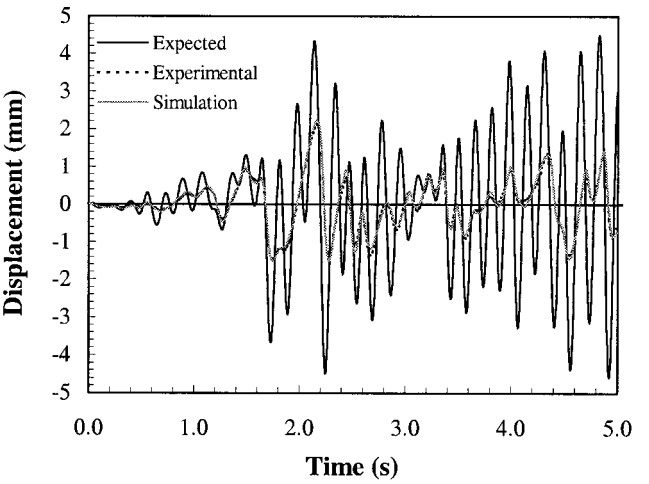

(b) Displacement response

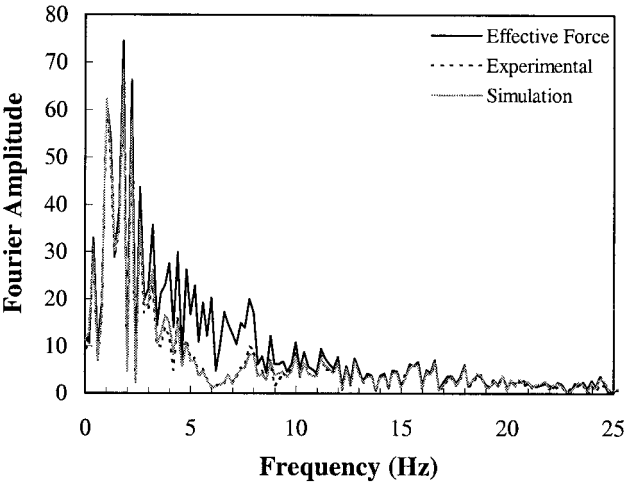

(c) Fast Fourier transforms of the effective force

FIG. 6. Expected, Experimental, and Simulation Results for El Centro Segment

insofar as producing an equivalent structural response. The first of these items is the most straightforward to address.

It is important that the applied earthquake motion be repeatable for situations in which more than one specimen is to be tested identically and the results compared. Fig. 4 includes two curves for the 1.9 L/s (30 gpm) servovalve, representing two tests using the same input effective forcing function (command signal), but at different times. The results are virtually identical. This demonstrates the repeatability of the EFT modified ground acceleration on the same test structure. However, this particular example does not ensure repeatability for two test specimens with different properties.

Reproducibility of the ground acceleration record was evaluated by investigating the test structure displacement response and the frequency content of the effective forcing function. Fig. 6 compares the expected response with the measured response for tests with the 5.7 L/s (90 gpm) servovalve for a 5 s segment of El Centro. The expected displacement histories [Fig. 6(b)] were calculated by solving the equation of motion using the respective ground acceleration and measured properties (mass, stiffness, damping) of the system. The measured displacement response was obtained from linear variable differential transformers (LVDTs) attached between the cart and the floor. In comparing the measured displacement histories with the expected response, it is evident that the input motion was not reproduced well.

To better understand these results, fast Fourier transforms (FFTs) were used to convert the forcing functions from the time domain to the frequency domain [Fig. 6(c)]. It is evident in the figures that the Fourier amplitude of the measured loading approached zero near the natural frequency of the SDOF model (6.3 Hz). This large difference in frequency response near the natural frequency of the SDOF system was responsible for the large difference observed between the measured and expected displacements [Fig. 6(b)].

Because insufficient oil supply (power) had been ruled out as the cause of the system's inability to apply the effective force command at frequencies near the natural frequency of the SDOF system tested, possible control problems were investigated.

Servohydraulic Control Problems

Problems with control-structure interaction have been identified by Dyke et al. (1995) in a study of active control of structures. They found that the natural velocity feedback loop that exists within the hydraulic actuator causes the performance of the actuator to be directly affected by the dynamics of the structure. They concluded that hydraulic actuators attached to undamped or lightly damped structures are greatly limited in their ability to apply forces near the natural frequency of the structure.

This can be shown through investigation of the block diagram given in Fig. 7. In the model of interaction between the actuator and the structure shown in Fig. 7, $G_a(s)$ represents the transfer function of the actuator. The response of the structure, y, to the applied force, f, is represented by the transfer function $G_{yf}(s)$. Finally, the transfer function $H_i(s)$ represents the natural velocity feedback that exists in hydraulic actuators.

Equilibrating the inputs to the outputs at the summing point of the block diagram model, the transfer function from the command signal, u, to the structural response, y, may be written as

$$G_{yu} = \frac{y}{u} = \frac{G_{yf}G_a}{1 + G_{yf}G_aH_i} \tag{7}$$

Similarly, the transfer function from the command signal, u, to the force applied to the structure, f, may be written as

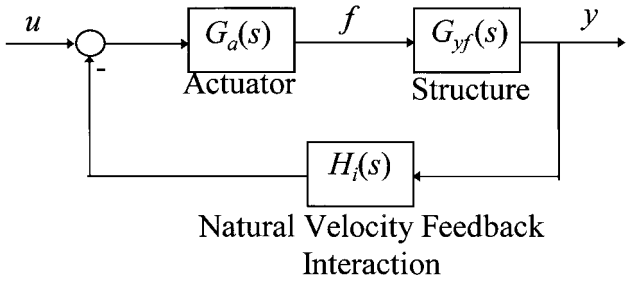

FIG. 7. Model of Interaction between Actuator and Structure (Dyke et al. 1995)

$$G_{fu} = \frac{f}{u} = \frac{G_a}{1 + G_{yf}G_aH_i} \tag{8}$$

Two important features of a transfer function are its poles and zeros. Poles are defined as those values of s where the denominator of the transfer function goes to zero. Zeros are defined as those values of s where the numerator goes to zero. If the transfer function has a zero at some value of s, then the output will be zero at this frequency. In order to better identify the poles and zeros of the transfer function described in (8), this equation may be written in terms of the numerator, $n(s)$, and denominator, $d(s)$, polynomials of each transfer function as follows:

$$G_{fu} = \frac{G_a}{1 + G_{yf}G_aH_i} = \frac{\dfrac{n_a}{d_a}}{1 + \dfrac{n_{yf}n_an_i}{d_{yf}d_ad_i}} = \frac{d_{yf}n_ad_i}{d_{yf}d_ad_i + n_{yf}n_an_i} \tag{9}$$

From (9), zeros of the transfer function, G_{fu}, from the input command, u, to the applied force, f, occur when d_{yf} is zero. By definition, these zeros are at the same frequencies as the poles of the transfer function for the structure ($G_{yf} = n_{yf}/d_{yf}$ is infinite).

In the case of the SDOF model as tested at the University of Minnesota, the transfer function from the applied force, f, to the displacement response of the structure, y, may be derived from (4) as

$$G_{yf} = \frac{n_{yf}}{d_{yf}} = \frac{1}{ms^2 + k} \tag{10}$$

where m and k are the mass and stiffness of the SDOF model, respectively. Damping, c, is neglected in this equation for simplicity. A pole of the transfer function for the structure ($d_{yf} = 0$) occurs at the natural frequency of the structure ($s = i\sqrt{k/m}$). It follows then that a zero of the transfer function $G_{fu}(s)$ occurs at the natural frequency of the structure. Thus an actuator attached to an undamped structure is unable to apply a force at the natural frequency of the structure, and an actuator attached to a lightly damped structure is greatly limited in its ability to apply forces at the natural frequency of the structure. This phenomenon explains the performance effects observed in Fig. 6.

COMPUTER SIMULATION STUDIES

Computer simulation studies were conducted using SIMULINK, dynamic simulation software within MATLAB, to investigate the entire dynamic system, including the servohydraulics and the test structure. Using the linearized hydraulic model shown in Fig. 8 and system parameters listed in Tables 1 and 2, computer simulation tests were conducted to verify the results obtained from the EFT studies conducted in the laboratory and to test possible solutions to the natural velocity feedback problem.

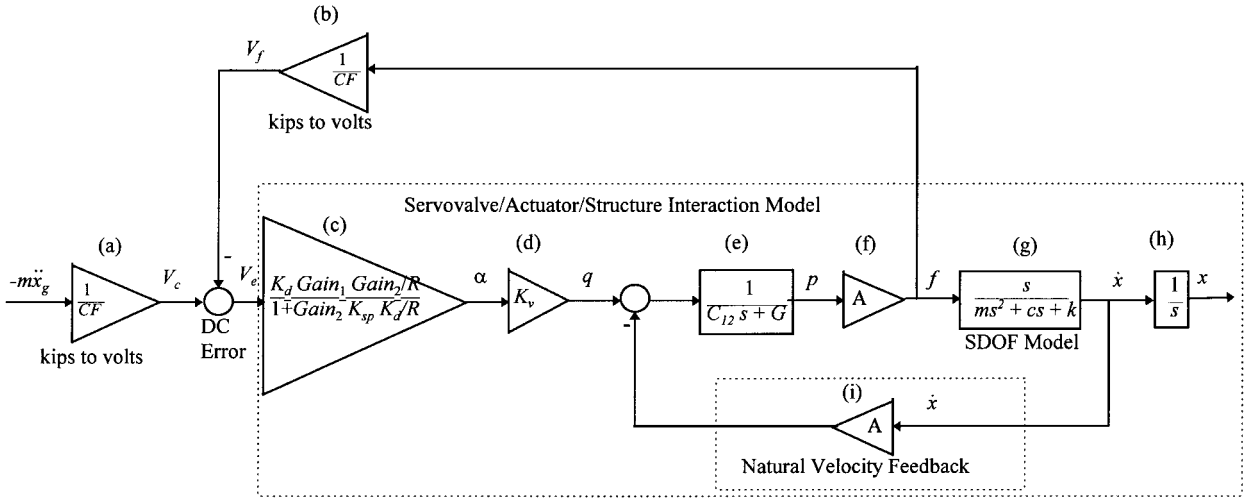

FIG. 8. Linearized Model of Dynamic System

TABLE 1. Model Properties

Parameter (1)	Value (2)
m	7,940 kg (0.045 kip s^2/in.)
k	11.8 kN/mm (67.1 kip/in.)
c	12.2 kN s/m (0.070 kip s/in.)
ζ	2% (2%)

TABLE 2. Actuator, Hydraulic, and Controller Properties

Parameter (1)	1.9 L/s (30 gpm) valve (2)	5.7 L/s (90 gpm) valve (3)
A	0.0174 m^2 (27.0 in.^{2})	0.0174 m^2 (27.0 in.^{2})
C_{12}	1.93×10^6 mm^5/kN (0.81 in.^{5}/kip)	1.93×10^6 mm^5/kN (0.81 in.^{5}/kip)
CF	0.028 V/kN (0.125 V/kip)	0.028 V/kN (0.125 V/kip)
G	0.00 m^5/kN s (0.00 in.^{5}/kip s)	0.00 m^5/kN s (0.00 in.^{5}/kip s)
$Gain_1$	5 V/V (5 V/V)	1.05 V/V (1.05 V/V)
$Gain_2$	1 V/V (1 V/V)	2 V/V (2 V/V)
K_{sp}	0 V/% (0 V/%)	0.1 V/% (0.1 V/%)
K_d	20.0 %/amp (20.0 %/amp)	20.0 %/amp (20.0 %/amp)
K_v	2.99×10^6 mm^3/s (182.6 in.^{3}/s)	8.98×10^6 mm^3/s (547.9 in.^{3}/s)
p_s	17.2 MPa (2,500 psi)	17.2 MPa (2,500 psi)
q_{max}	2.99×10^6 mm^3/s (182.6 in.^{3}/s)	8.98×10^6 mm^3/s (547.9 in.^{3}/s)
R	200 Ω (200 Ω)	200 Ω (200 Ω)
β	686 MPa (100 ksi)	686 MPa (100 ksi)

The blocks of Fig. 8 are labeled with letters $a-i$ to aid in explanation of the model. Block *a* represents conversion of the input effective forcing function (command signal) from units of kips to volts. This command signal (V_c) is then compared with the feedback signal from the actuator load cell (V_f), which is converted from kips to volts in block *b*. The difference between the two signals is the error signal (V_e).

The interaction model between the servovalve/actuator and the test structure (SDOF model) is shown within the larger dashed box of Fig. 8 (blocks $c-i$). The error signal goes through a stage where it is converted from voltage to servovalve opening, as shown in block *c*. The constants in this stage are dependent on the type of servovalve used. For a two-stage valve [e.g., 1.9 L/s (30 gpm)], block *c* reduces to $K_d\, Gain_1/R$ ($Gain_2 = 1$, $K_{sp} = 0$). $Gain_1$ is the user-set gain on the controller. The resistance ($1/R$) converts the voltage to current, and the mechanical gain (K_d) converts the current to spool opening. All tests performed in this study had operating frequencies well below 30 Hz, the upper limit for which the current signal is linearly related to the valve spool opening (by K_d) for the MTS servovalves used in the tests. The mechanical gain (K_d) was found by relating full-scale values as follows:

$$K_d = \frac{\alpha_{max}}{i_{max}} \tag{11}$$

where α_{max} is the full-scale spool opening and i_{max} is the full-scale current. For a three-stage valve [e.g., 5.7 L/s (90 gpm)], the controller provides an extra gain stage, with an inner feedback loop, which has been replaced by its equivalent gain in Fig. 8. The two additional parameters used for the three-stage valve are the spool gain (K_{sp}), which converts spool opening to voltage in the servovalve feedback loop, and the servovalve inner loop gain ($Gain_2$), which is user set on the controller. The spool gain (K_{sp}) was found by relating the full-scale spool opening (α_{max}) to the full-scale spool LVDT voltage ($V_{sp-LVDT_{max}}$):

$$K_{sp} = \frac{\alpha_{max}}{V_{sp-LVDT_{max}}} \tag{12}$$

The flow through the servovalve is a nonlinear function of both the valve spool opening and the pressure drop across the servovalve as given in (5). This equation can be inverted and rewritten in terms of oil flow, q, and pressure across the actuator piston, p_l:

$$\frac{q}{q_{max}} = \alpha \sqrt{1 - \text{sgn}(\alpha)\, \frac{p_l}{p_s}} \tag{13}$$

where q_{max} is the maximum flow with full effective supply pressure drop across the servovalve, and p_s is the hydraulic supply pressure. To simplify the model, (13) describing oil flow through the servovalve was linearized as

$$q = K_v \alpha - G_v p_l \tag{14}$$

where K_v is the flow gain and G_v is the flow-pressure coefficient, or valve ''leakage'' (Merritt 1967). The values of K_v and G_v vary depending on the operating point. For the purposes of this study, the linearization was performed about the null operating point. At the null operating point, G_v is approximately equal to zero and is therefore neglected in the simulation model. The value of K_v at the null operating point is the no-load flow gain. This value can be found by setting p_l equal to zero in (13), which results in

$$q = q_{max} \alpha \tag{15}$$

At the null operating point, the constant K_v relating the spool

opening to flow is equivalent to q_{max}. This relation is represented by block *d* in the model.

The transfer function of block *e* in Fig. 8 translates the flow to pressure. This conversion is a function of the compressibility of the oil and the actuator leakage. Depending on the direction in which the servovalve spool opens, pressure is applied to one side of the piston and the other side is open to the return line. The differential pressure acting over the cross-sectional area of the piston produces the applied force. The flow into the actuator produces a change in the oil pressure in the actuator and causes the piston to move as described by the following linearized equation:

$$q = C_{12}\dot{p}_l + G_1 p_l + A\dot{x} \tag{16}$$

where C_{12} is the oil compressibility constant, G_1 is a constant representing the actuator leakage, A is the cross-sectional area of the actuator piston, $\dot{x}$ is the piston velocity, and $\dot{p}_l$ is the derivative of the pressure drop across the actuator with respect to time (Merritt 1967). Block *f* represents the translation of pressure across the piston to force provided by the actuator by multiplying the differential pressure by the cross-sectional area of the piston. The constant G in block *e* is the sum of the actuator leakage (G_1) and the valve leakage (G_v). Both of these leakage flows were neglected in the simulation model (G was set equal to zero) because the leakage was negligible for the servovalves and the frequency ranges employed in the tests. The oil compressibility constant may be approximated as

$$C_{12} = \frac{V}{4\beta} \tag{17}$$

where V is the total volume of both chambers of the actuator, and β is the bulk modulus of the fluid. The total volume V is assumed to be equal to the cross-sectional area of the piston times the stroke capacity of the actuator.

The final term of (16) represents the natural velocity feedback that exists within the actuator, shown in block *i* of Fig. 8. The force produced by the actuator is partially dependent on the velocity of the actuator piston. The interaction of the actuator with the test structure arises because the motion of the actuator piston, both displacement and velocity, is dependent on the response of the test structure to the applied force; the velocity of the actuator piston will be equal to the velocity of the structure at the point where the actuator is attached. The transfer function describing the velocity response of the test structure (SDOF model) to the applied force is shown in block *g* of Fig. 8. This transfer function was derived from (4) for the response of a SDOF system to an external force applied through the center of mass. The velocity response of the test structure was integrated (shown in block *h*) to obtain the displacement response of the test structure.

A physical explanation of the natural velocity feedback follows. As pressure is applied to the piston, the piston moves according to the response of the attached test structure. The slightest movement of the piston increases the volume of the chamber on the pressure side of the piston so that additional oil flow into the chamber is required to maintain the same pressure on the piston. The oil flow continuously has to compensate for the increasing volume of the pressure chamber, which is directly related to the response of the test structure (SDOF model). Consequently, the actual oil flow into the actuator resulting in pressure applied to the piston continuously falls short of the flow needed to produce the command force. This phenomenon is exacerbated at the natural frequency of the test structure by resonance.

Results of Initial Simulation Tests

Results of the numerical simulation study using SIMULINK conducted on the linearized model (Fig. 8) are shown in Fig. 6 with the expected and measured results for the 5 s segment of El Centro. It is evident that the dynamic simulation results replicated the experimental results, confirming that the linearized model developed to represent the servohydraulics and SDOF structure was an accurate representation of the system. The simulation tests corroborated the actuator's inability to apply forces at the natural frequency of the SDOF model because of the velocity feedback of the system.

One Solution to Natural Velocity Feedback Problem

The natural velocity feedback causes the control of the actuator to be affected by the response of the structure; consequently the actuator is unable to apply force near the natural

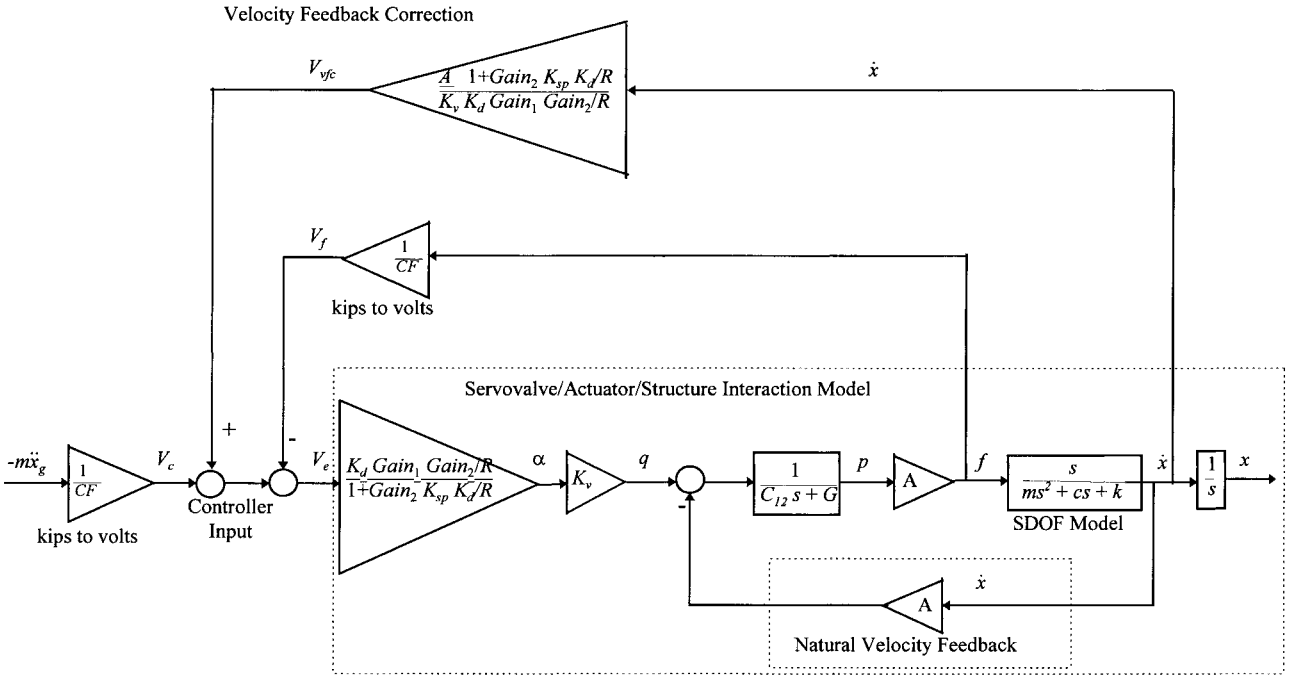

FIG. 9. Linearized Model of Dynamic System Incorporating Velocity Feedback Correction Loop

frequency of the structure. A possible solution is to create an additional feedback loop to negate the effect of the natural velocity feedback. The key to implementing this solution is being able to accurately determine the transfer function for this correction.

An inspection of Fig. 8 indicates that the ideal means of negating the natural velocity feedback loop would be to measure the velocity response of the SDOF model, multiply the velocity times the piston area, and add the resulting flow value to the flow into the actuator. However, this approach is not physically feasible. The easiest way to alter the flow into the actuator is through the command signal to the controller. Fig. 9 presents a block diagram of the velocity feedback correction implementation for the linearized hydraulic model. The velocity response of the SDOF is measured and a series of conversions (velocity to flow, flow to spool opening, spool opening to voltage) are performed to generate a voltage signal, denoted by V_{vfc}, that may be added to the command signal. These conversions are independent of the test structure and consist only of constants for the linearized model. Therefore, experimental implementation of this scheme is conceptually simple. A velocity transducer could be used to measure the response of the SDOF model. The analog signals from the velocity transducer could then be amplified according to the predetermined correction constant and added to the command signal by means of a summing amplifier.

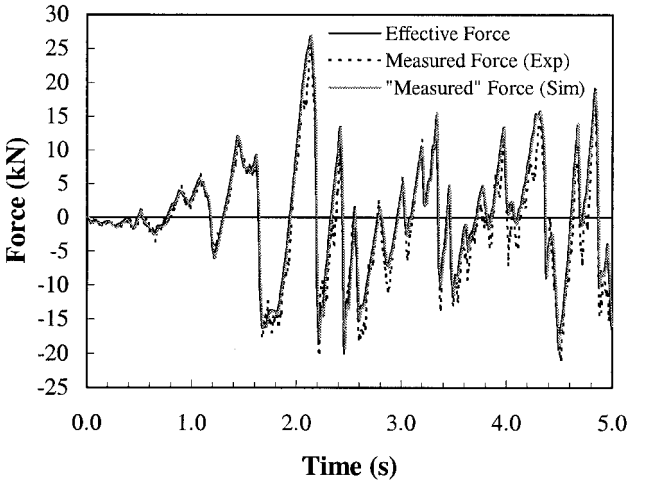

(a) Effective force

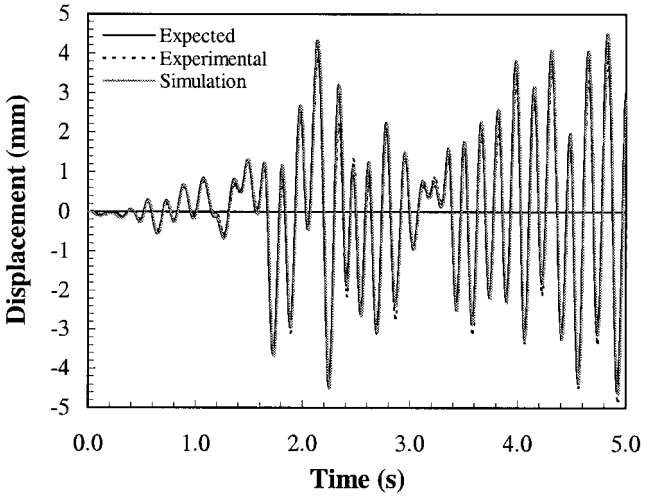

(b) Displacement response

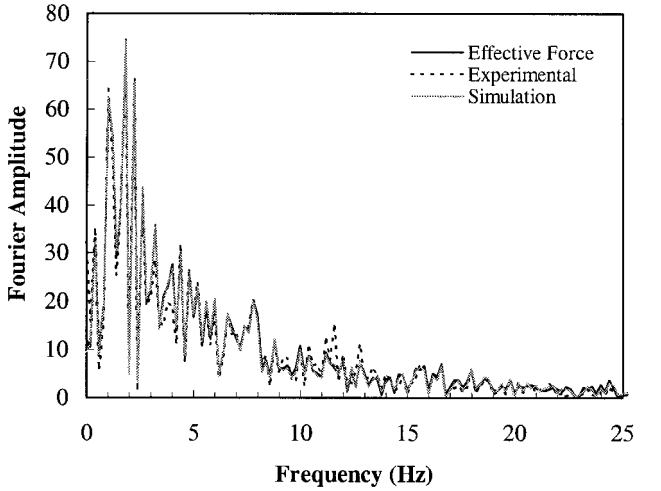

(c) Fast Fourier transforms of the effective force

FIG. 10. Expected, Precorrected, and Simulation (Incorporating Velocity Feedback Correction) Results for El Centro Segment

The SIMULINK model with the assumed linearized servovalve/actuator model and measured structural properties confirmed that this method should eliminate problems with velocity feedback. To test the proposed feedback scheme experimentally, a ''precorrected'' command signal was input to the controller. Rather than measuring the velocity and applying the feedback correction in real time, the expected velocity was calculated by solving the equations of motion for the linear elastic SDOF structure. The precorrected command signal was then obtained by multiplying the expected velocity history by the correction constant discussed in the previous paragraph and then summing this new time series with the original effective force record. Fig. 10 shows the results of applying the precorrected signal to the SIMULINK model and to the actual test structure. In both cases, the measured force from simulation and measured force from the experiment showed good agreement with the effective force ($-m\ddot{x}_g$) in both the time and frequency domains [Figs. 10(a and c)], especially around the natural frequency of structure. The simulation and measured displacements also correlated well with the expected results [Fig. 10(b)], in contrast to the system without the velocity feedback correction [Fig. 6(b)]. Further studies were successfully conducted using the measured velocity to supply the velocity feedback correction. A complete description of the experimental implementation is to appear in an article (''Experimental implementation of velocity feedback correction for effective force testing'') being prepared by J. Timm, C. Shield, and C. French.

For the experimental and simulation tests in which the El Centro segment effective force was applied to the SDOF model, the force required was well within the force capacity of the actuator, as shown in Fig. 5. For this reason, the linear model was a fairly accurate representation of the 340 kN−1.9 L/s (77 kip−30 gpm) system in simulating the El Centro segment effective force.

Incorporating Nonlinearities into Correction Loop

In certain situations, it may be required to incorporate servovalve/actuator nonlinearities. Although in the tests described above, the linear model was adequate, the flow through the servovalve is a nonlinear function of both the spool opening and the pressure across the actuator as presented in (13). This nonlinearity is most severe when the system is operated near the force capacity of the actuator as shown in Fig. 5 containing the force-velocity curves for the actuator.

To more accurately model the system performance in such cases, it is possible to incorporate nonlinearities such as the force-velocity relationship into both the dynamic system

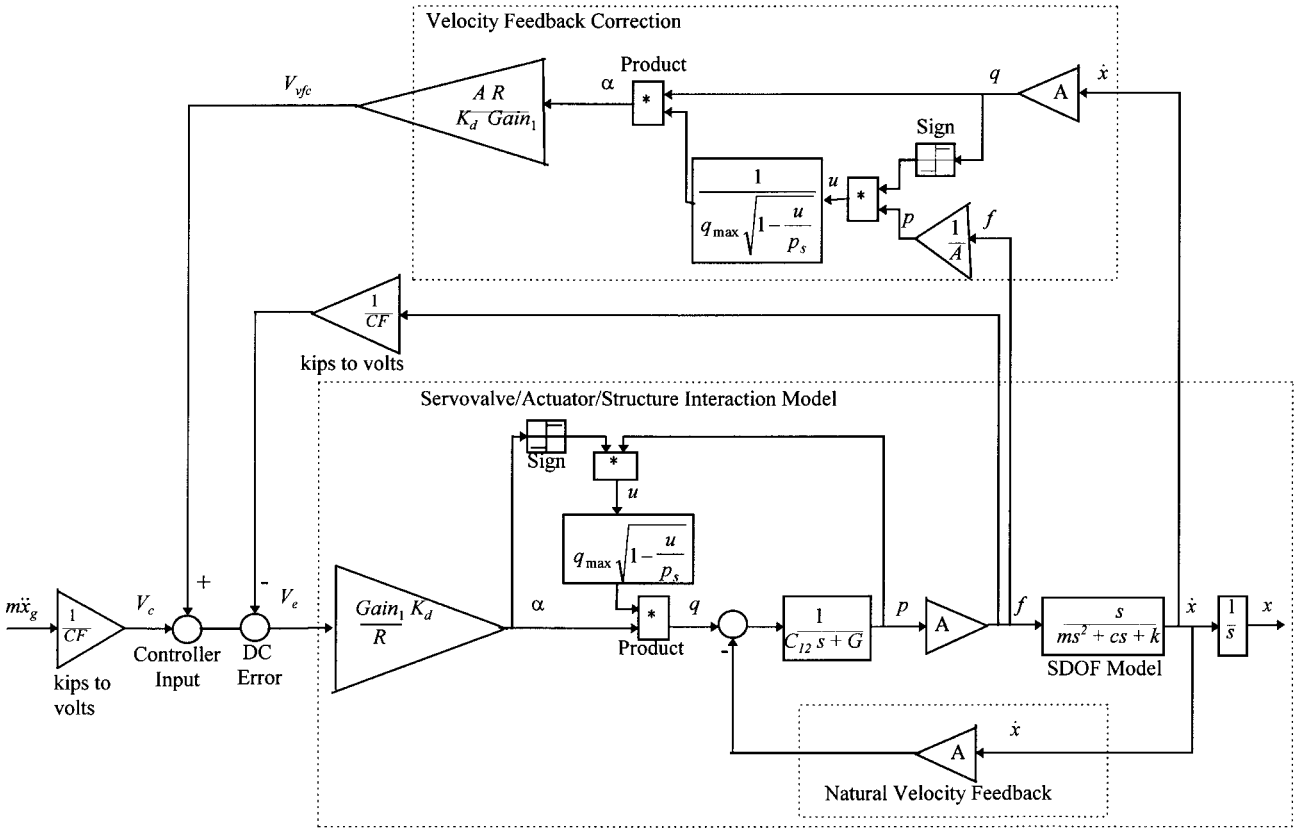

FIG. 11. Model of Dynamic System Incorporating Nonlinear Relationship Describing Two-Stage Servovalve Flow

model and the velocity feedback correction loop. In Fig. 11, the constant K_v, relating spool opening to oil flow through the servovalve in the linearized model for a two-stage servovalve, has been replaced by the nonlinear relationship of (13). The product of the pressure, p, and the sign of the spool opening (negative = −1, positive = +1, zero = 0) is fed into a block to calculate the value relating the spool opening, α, and the flow, q, according to (13). The output of this block is then multiplied by the spool opening, α, to obtain the flow, q, into the actuator. With this nonlinearity incorporated into the model, developing a feedback loop to negate the natural velocity feedback becomes more complex (also shown in Fig. 11). Because the flow is now dependent on both the spool opening and the pressure across the actuator, the reverse conversion from flow to spool opening is not simply $1/K_v$, as it was for the linearized model. Instead, the measured force from the actuator load cell must be used to relate flow to spool opening according to (13). Although some of the feedback parameters are no longer simple gains, as was the case for the linearized model, the feedback conversion parameters are still independent of the test structure.

Although experimental implementation of the nonlinear velocity feedback correction is more complex than for the linear case, it is still possible. Analog or digital circuits can be used to manipulate the signals from the velocity transducer on the structure and from the actuator load cell in order to generate the desired correction voltage (V_{vfc}) to add to the effective force time series. As for the linear case, the ability to negate the natural velocity feedback depends on how accurately the parameters within the correction loop represent the actual system.

CONCLUSIONS

The effective force testing (EFT) method shows promise as a method that can be used to complement existing earthquake simulation models (i.e., quasi-static, pseudodynamic, and shake table tests). EFT employs a force control algorithm that enables real-time earthquake simulation studies of large-scale structures.

The potential of the method was investigated with numerical simulation and experimental studies using an SDOF system. To evaluate the earthquake simulation produced by the actuator, the frequency response of the measured force was compared with the frequency response of the effective force ($-m\ddot{x}_g$). In its most straightforward application, for the effective force commands input directly to the controller, the FFT of the measured force approached zero near the natural frequency of the SDOF model. This was especially evident in the case of the effective force segment from the El Centro ground motion, which had a large spike in the FFT near the natural frequency of the structure. In which case, the actuator was unable to excite the SDOF model at its natural frequency.

The results of the experimental tests and simulation studies correlated with the conclusions drawn by Dyke et al. (1995) that hydraulic actuators have a limited ability to apply forces at the natural frequency of lightly damped structures. This is due to the interaction of the actuator and the structure through the natural velocity feedback of the actuator. One possible solution to the natural velocity feedback problem is to create an additional feedback loop to negate the natural velocity feedback of the actuator. Results of simulation and experimental tests that compensated for the anticipated velocity feedback indicated that the effective force can be accurately applied to the test structure regardless of the frequency content of the loading.

ACKNOWLEDGMENTS

Funding for this project was provided by the National Science Foundation under Grant NSF/GER-9023596. The writers would also like to acknowledge the materials and labor donated by GCR Truck Tire Center.

APPENDIX I. REFERENCES

Chopra, A. K. (1995). *Dynamics of structures: Theory and applications to earthquake engineering*. Prentice-Hall, Englewood Cliffs, N.J., 20–22.

Clark, A. J. (1983). ''Sinusoidal and random motion analysis of mass loaded actuators and valves.'' *Proc., Nat. Conf. on Fluid Power*.
Clark, A., French, C. W., and Leon, R. T. (1989). ''Earthquake testing methods for structures: Examples of current practice and future directions.'' *Earthquake research construction and design*, S. A. Savidis, ed., A. A. Balkema, Rotterdam, The Netherlands, 409–418.
Clough, R. W., and Penzien, J. (1975). *Dynamics of structures*. McGraw-Hill, New York, 546.
Dyke, S. J., Spencer, B. F., Quast, P., and Sain, M. K. (1995). ''Role of control-structure interaction in protective system design.'' *J. Engrg. Mech.*, ASCE, 121(2), 322–338.
Mahin, S. A., and Shing, P. B. (1985). ''Pseudodynamic method for seismic testing.'' *J. Struct. Engrg.*, ASCE, 111(7), 1482–1503.
Mahin, S. A., Shing, P. B., Thewalt, C. R., and Hanson, R. D. (1989). ''Pseudodynamic test method—Current status and future directions.'' *J. Struct. Engrg.*, ASCE, 115(8), 2113–2128.
Merritt, H. E. (1967). *Hydraulic control systems*. Wiley, New York.
Moehle, J. P., ed. (1996). *Earthquake spectra—Theme issue: Experimental methods*. Earthquake Engineering Research Institute, El Cerrito, Calif.
Murcek, J. A. (1996). ''Evaluation of the effective force testing method using a SDOF model,'' MS thesis, University of Minnesota.
Nakashima, M., Kato, H., and Takaoka, E. (1992). ''Development of real-time pseudo dynamic testing.'' *Earthquake Engrg. and Struct. Dynamics*, 21, 79–92.
Thewalt, C. R., and Mahin, S. A. (1987). ''Hybrid solution techniques for generalized pseudodynamic testing.'' *Rep. UBC/EERC-87/09*, EERC, University of California, Berkeley.

APPENDIX II. NOTATION

The following symbols are used in this paper:

A = cross-sectional area of actuator piston;
C_{12} = oil compressibility constant;
c = viscous damping coefficient of single-degree-of-freedom system;
d_γ = denominator of transfer function G_γ or H_γ;
f, $f_{\max}$ = actuator force and maximum rated force of actuator;
G_1, G_v, G = leakage coefficients for actuator and valve, and sum of leakage coefficients;
G_a, $G_{\zeta\gamma}$ = transfer functions;
H_i = natural velocity feedback transfer function;
i = current signal;
K_d, K_v = mechanical and flow gains;
k = stiffness of single-degree-of-freedom system;
k_s = servovalve flow rating;
m = mass of single-degree-of-freedom system;
n_γ = numerator of transfer function G_γ or H_γ;
p_d, p_l, p_s = pressure drop across orifice, pressure across piston in actuator, supply pressure;
p_{eff} = effective force;
q, $q_{\max}$ = oil flow and maximum flow into actuator with full effective pressure drop across servovalve;
R = controller resistance;
s = Laplace variable;
u = drive signal sent from controller;
V = total volume of both chambers of actuator;
V_c, V_e, V_f, V_{vfc} = command signal, error signal, feedback signal, and velocity feedback ''correction'' voltages;
$V_{\text{sp}-\text{LVDT}_{\max}}$ = maximum voltage output of spool LVDT;
v, $v_{\max}$ = velocity and maximum velocity of actuator piston;
x, $\dot{x}$, $\ddot{x}$ = displacement, velocity, and acceleration relative to ground;
x_a, $\ddot{x}_a$ = absolute displacement and acceleration;
x_g, $\ddot{x}_g$ = ground displacement and ground acceleration;
α, $\alpha_{\max}$ = servovalve and maximum servovalve spool opening; and
β = bulk modulus of fluid.